6th European Conference on Computational Mechanics (ECCM 6)
7th European Conference on Computational Fluid Dynamics (ECFD 7)
1115 June 2018, Glasgow, UK

AN ANISOTROPIC DAMAGE AND FRACTURE MODEL BASED ON A SECOND ORDER DAMAGE TENSOR

M. FASSIN[1], R. EGGERSMANN[1], S. WULFINGHOFF[1] AND S. REESE[1]

[1] Institute of Applied Mechanics, RWTH Aachen University
Mies-van-der-Rohe-Str.1, 52074 Aachen (Germany)
marek.fassin@rwth-aachen.de, www.ifam.rwth-aachen.de

Key words: anisotropic damage, damage growth, thermodynamical consistency

Abstract. The present work deals with an elastic anisotropic damage model which utilizes a damage tensor of second order. The considered class of materials is characterized by an initially isotropic quasi-brittle material behaviour. Artificial stiffening effects during damage processes are excluded by the specific choice of the elastic part of the free energy. Based on the Helmholtz free energy the model equations are derived in a thermodynamically consistent way. In order to ensure that the eigenvalues of the damage tensor do not exceed the value one, anisotropic damage hardening is introduced. Two approaches, (i) a suddenly increasing function and (ii) a smooth function are proposed and discussed in detail. It is shown exemplarily with a uniaxial loading that the latter one performs well, where the former one suffers from a second (undesired) elastic region. Two more numerical examples are investigated in order to illustrate the behaviour of the model for two- and three-dimensional loading scenarios.

1 INTRODUCTION

Since the pioneering work of Kachanov [1] in 1958 continuum damage mechanis has emerged as an important field in continuum mechanics. Introducing damage as a scalar variable is a simplifying assumption but still today many constitutive models utilize a scalar damage variable (being equivalent to isotropic damage). However, from the physical point of view it seems to be reasonable to model damage anisotropic, e.g. the orientation of microcracks may be dependent on the loading direction and/or preferred directions of the materials. A simple possibility to model anisotropic damage is to use multiple scalar damage variables (see e.g. [2] for a microplane model). It seems to be easy to model damage by a vector (see for an exemplary model [3]), but unfortunately damage tensors of odd-order have essential limitations and furthermore, the effect of total damage cannot be expressed by the sum of the damage vectors of each plane. Modeling damage with a damage tensor of second order (see e.g. [4]) is already a quite sophisticated approach, nevertheless anisotropic damage is restricted to orthotropic degradation, cf. the discussion in [5]. Though, orthotropic degradation seems to be sufficient for many applications. For the numerical implementation of an anisotropic damage model coupled to plasticity using

a second order damage tensor, see [6, 7]. More complex models even work with a damage tensor of fourth order (see e.g. [8]), where the fourth order tensor maps between the effective stress tensor and the cotinuum mechanical stress tensor (both tensors of second order). Ultimately, anisotropic damage can be represented by a damage tensor of eighth order. This tensor of eighth order then maps between the undamaged (virgin) stiffness and the damaged stiffness (both tensors of fourth order).
The present paper utilizes a damage tensor of second order, where the elastic part of the free energy is constructed in such a way that the model a priori excludes artificial stiffening effects. In order to show this mathematically, Wulfinghoff et al. [9] derived a criterion, called the damage growth criterion, which has to be fulfilled to exclude artificial stiffening effects. Or in other words, if this criterion is fulfilled, it is guaranteed that during any damage process the material's stiffness decreases (or at least remains constant) in each direction.

2 MODEL EQUATIONS

In this work, an elastic anisotropic damage model using a second order damage tensor is presented. Initially isotropic materials are considered and the geometrically linear theory is applied utilizing the infinitesimal strain tensor $\boldsymbol{\varepsilon} = \mathrm{sym}(\nabla \boldsymbol{u})$, where $\boldsymbol{u}$ denotes the displacement field.

2.1 Helmholtz free energy

Starting point of the constitutive model is the Helmholtz free energy which is assumed to take the form

$$\psi \;\; = \psi_{\mathrm{e}}(\boldsymbol{\varepsilon}, \boldsymbol{D}) + \psi_{\mathrm{h}}^{\mathrm{iso}}(\alpha) + \psi_{\mathrm{h}}^{\mathrm{ani}}(\boldsymbol{D}) \tag{1}$$

The elastic part of the free energy is represented by ψ_{e} and depends on the strain tensor $\boldsymbol{\varepsilon}$ and the symmetric second order damage tensor $\boldsymbol{D}$ (six independent components). Furthermore, isotropic damage hardening represented by $\psi_{\mathrm{h}}^{\mathrm{iso}}$ (being dependent on the damage hardening variable α) and anisotropic damage hardening ($\psi_{\mathrm{h}}^{\mathrm{ani}}$) are considered. A specific form of the elastic free energy function for initially isotropic materials which excludes artificial stiffening effects a priori is adopted from [11]

$$\psi_{\mathrm{e}}(\boldsymbol{\varepsilon}, \boldsymbol{D}) = \underbrace{\tfrac{1}{2}\big(1-g\big)\lambda\,\mathrm{tr}^2(\boldsymbol{\varepsilon})}_{\lambda\text{-term}} + \underbrace{\mu\big(\boldsymbol{I}-\boldsymbol{D}\big) : \boldsymbol{\varepsilon}^2}_{\mu\text{-term}} \tag{2}$$

Here, λ and μ denote the Lamé parameters. As can be seen, the λ-term is damaged isotropic by the scalar $(1-g)$, where g is a function of the trace of the damage tensor: $g = g(\mathrm{tr}(\boldsymbol{D}))$. A simple choice for the g-function is $g(\mathrm{tr}(\boldsymbol{D}))=\frac{1}{3}\,\mathrm{tr}(\boldsymbol{D})$ which will be used in the following. The isotropic damage hardening energy is chosen to be quadratic in the damage hardening variable α

$$\psi_{\mathrm{h}}^{\mathrm{iso}}(\alpha) \;\; = \;\; \tfrac{1}{2}K_1\alpha^2 \tag{3}$$

Clearly, more complex hardening energies (such as exponential hardening) can be considered. In the context of initially isotropic materials, anisotropic damage hardening does not seem to be of importance. However, using a second order damage tensor implies the problem that eigenvalues of the damage tensor may exceed the value of one which would be nonphysical. To avoid this situation the anisotropic damage hardening is utilized. Making the anisotropic damage hardening dependent on the eigenvalues D_i of the damage tensor $\boldsymbol{D}$

$$\psi_{\mathrm{h}}^{\mathrm{ani}}(\boldsymbol{D}) = \sum_{i=1}^{3} f(D_i) \tag{4}$$

the eigenvalues can be bounded, which will be discussed later on in detail. Next, the second law of thermodynamics is considered in order to derive the thermodynamic conjugate forces from the Helmholtz free energy defined in this section.

2.2 Second law of thermodynamics and thermodynamic conjugate forces

The second law of thermodynamics states that the dissipation within the material has to be always nonnegative. Neglecting thermal effects, that means that the mechanical energy stored within the material (consisting of a reversible and an irreversible part) can not exceed the mechanical work generated on the material. The second law of thermodynamics (dissipation inequality) then reads

$$\mathcal{D} = \boldsymbol{\sigma} : \dot{\boldsymbol{\varepsilon}} - \dot{\psi} \geq 0 \tag{5}$$

Inserting the expressions for the free energy in Eq. (5) yields

$$\begin{aligned}
\mathcal{D} &= \boldsymbol{\sigma} : \dot{\boldsymbol{\varepsilon}} - \left[\frac{\partial \psi}{\partial \boldsymbol{\varepsilon}} : \dot{\boldsymbol{\varepsilon}} + \frac{\partial \psi}{\partial \boldsymbol{D}} : \dot{\boldsymbol{D}} + \frac{\partial \psi}{\partial \alpha} \dot{\alpha} \right] \\
&= \boldsymbol{\sigma} : \dot{\boldsymbol{\varepsilon}} - \left[\frac{\partial \psi_{\mathrm{e}}}{\partial \boldsymbol{\varepsilon}} : \dot{\boldsymbol{\varepsilon}} + \left(\frac{\partial \psi_{\mathrm{e}}}{\partial \boldsymbol{D}} + \frac{\partial \psi_{\mathrm{h}}^{\mathrm{ani}}}{\partial \boldsymbol{D}} \right) : \dot{\boldsymbol{D}} + \frac{\partial \psi_{\mathrm{h}}^{\mathrm{iso}}}{\partial \alpha} \dot{\alpha} \right] \\
&= \underbrace{\left(\boldsymbol{\sigma} - \frac{\partial \psi_{\mathrm{e}}}{\partial \boldsymbol{\varepsilon}} \right) : \dot{\boldsymbol{\varepsilon}}}_{\text{term1}} - \Bigg[\underbrace{\left(\frac{\partial \psi_{\mathrm{e}}}{\partial \boldsymbol{D}} + \frac{\partial \psi_{\mathrm{h}}^{\mathrm{ani}}}{\partial \boldsymbol{D}} \right)}_{=-\boldsymbol{Y}} : \dot{\boldsymbol{D}} + \underbrace{\frac{\partial \psi_{\mathrm{h}}^{\mathrm{iso}}}{\partial \alpha}}_{=-\beta} \dot{\alpha} \Bigg] \geq 0
\end{aligned} \tag{6}$$

Usually, all dissipative mechanisms are associated with a change of the internal variables (here: $\boldsymbol{D}$ and α). Considering a virtual state where the internal variables $\boldsymbol{D}$ and α are fixed/freezed (i.e. $\dot{\boldsymbol{D}} = \boldsymbol{0}$ and $\dot{\alpha} = 0$), the dissipation has to vanish. Therefore, term 1 in Eq. (6) has to vanish independent of the value of $\dot{\boldsymbol{\varepsilon}}$. This is equivalent to the constitutive assumption

$$\boldsymbol{\sigma} = \frac{\partial \psi_{\mathrm{e}}}{\partial \boldsymbol{\varepsilon}} \tag{7}$$

stating that the stress $\boldsymbol{\sigma}$ and the strain $\boldsymbol{\varepsilon}$ are thermodynamic conjugate. Inserting Eq. (2) gives the specific expression for the stress tensor

$$\boldsymbol{\sigma} = \frac{\partial \psi_\mathrm{e}}{\partial \boldsymbol{\varepsilon}} = \underbrace{\big(1 - \tfrac{1}{3}\operatorname{tr}(\boldsymbol{D})\big)\lambda \operatorname{tr}(\boldsymbol{\varepsilon})\boldsymbol{I}}_{\boldsymbol{\sigma}_\lambda} + \underbrace{\mu\Big[\big(\boldsymbol{I} - \boldsymbol{D}\big)\boldsymbol{\varepsilon} + \boldsymbol{\varepsilon}\big(\boldsymbol{I} - \boldsymbol{D}\big)\Big]}_{\boldsymbol{\sigma}_\mu} \tag{8}$$

As already observed for the expression for the elastic part of the free energy, $\boldsymbol{\sigma}_\lambda$ is damaged in an isotropic and $\boldsymbol{\sigma}_\mu$ in an anisotropic manner. In the following the thermodynamic conjugate forces of $\boldsymbol{D}$ and α are discussed. The thermodynamically conjugate quantity of the damage tensor $\boldsymbol{D}$ is called damage driving force and is defined as

$$\boldsymbol{Y} = -\frac{\partial \psi_\mathrm{e}}{\partial \boldsymbol{D}} - \frac{\partial \psi_\mathrm{h}^\mathrm{ani}}{\partial \boldsymbol{D}} \tag{9}$$

It consists of two parts, where the first part is denoted by $\boldsymbol{Y}_\mathrm{e}$ and is given by

$$\boldsymbol{Y}_\mathrm{e} = -\frac{\partial \psi_\mathrm{e}}{\partial \boldsymbol{D}} = \underbrace{\tfrac{1}{6}\lambda \operatorname{tr}^2(\boldsymbol{\varepsilon})\boldsymbol{I}}_{=\boldsymbol{Y}_\lambda^\mathrm{e}} + \underbrace{\mu\,\boldsymbol{\varepsilon}^2}_{=\boldsymbol{Y}_\mu^\mathrm{e}} \tag{10}$$

It turns out that for the chosen ψ_e the damage tensor is not involved anymore in Eq. (10). The anisotropic damage hardening force is defined as follows

$$\boldsymbol{Y}_\mathrm{h}^\mathrm{ani} = \frac{\partial \psi_\mathrm{h}^\mathrm{ani}}{\partial \boldsymbol{D}} \tag{11}$$

where the definition of $\boldsymbol{Y}_\mathrm{h}^\mathrm{ani}$ as positive derivative and $\boldsymbol{Y}_\mathrm{e}$ as negative derivative (cf. Eq. (10)) lead to the resulting damage driving force given by

$$\boldsymbol{Y} = \boldsymbol{Y}_\mathrm{e} - \boldsymbol{Y}_\mathrm{h}^\mathrm{ani} \tag{12}$$

As explained above, the reason for the introduction of the anisotropic damage hardening is to ensure that the eigenvalues of the damage tensor do not exceed the value of one. For this reason it makes sense to reduce the damage driving force in the directions where the corresponding eigenvalues D_i of the damage tensor approach the value one. Hence, $\boldsymbol{Y}_\mathrm{h}^\mathrm{ani}$ is subtracted from $\boldsymbol{Y}_\mathrm{e}$. Two approaches for the anisotropic damage hardening are investigated:

$$\boldsymbol{Y}_{\mathrm{h},1}^\mathrm{ani} = \sum_{i=1}^{3} \underbrace{H_{\mathrm{h},1}^\mathrm{ani}\big\langle D_i - D_0\big\rangle}_{Y_{\mathrm{h},1}^\mathrm{ani}} \underbrace{\boldsymbol{n}_i^\mathrm{D} \otimes \boldsymbol{n}_i^\mathrm{D}}_{\boldsymbol{N}_i^D} \tag{13}$$

$$\boldsymbol{Y}_{\mathrm{h},2}^\mathrm{ani} = \sum_{i=1}^{3} \underbrace{H_{\mathrm{h},2}^\mathrm{ani}\frac{D_i}{\sqrt[n]{1 - D_i}}}_{Y_{\mathrm{h},2}^\mathrm{ani}} \underbrace{\boldsymbol{n}_i^\mathrm{D} \otimes \boldsymbol{n}_i^\mathrm{D}}_{\boldsymbol{N}_i^D} \tag{14}$$

The first approach given by Eq. (13) utilizes the Macaulay brackets being defined as

$\langle x \rangle = (x + |x|)/2$. This approach is a straightforward extension of the penalty energy used in Fassin et al. [10] for an isotropic damage model. The penalty parameter $H^{\text{ani}}_{\text{h},1}$ is usually chosen as high value (e.g. $H^{\text{ani}}_{\text{h},1} \geq 10^4$ Nmm/mm^3). If all eigenvalues D_i are below the critical damage value D_0 (which is typically chosen to be close to one, e.g. 0.99999) the anisotropic damage hardening remains zero. Once one of the eigenvalues has exceeded D_0 the anisotropic damage hardening force suddenly increases. A schematic illustration of the suddenly increasing function $\boldsymbol{Y}^{\text{ani}}_{\text{h},1}$ is depicted in Fig. 1a. The second investigated approach $\boldsymbol{Y}^{\text{ani}}_{\text{h},2}$ uses a smooth function which already slowly increases for small values of D_i, cf. Fig. 1b. Hence anisotropic damage hardening is present right from the beginning. Since the suggested function $\boldsymbol{Y}^{\text{ani}}_{\text{h},2}$ tends to infinity for $D_i \to 1$, the function is replaced from point (D_r, Y_r) by its tangent having the slope m_r. But this is only a numerical detail. The key point is that the second approach uses a smooth function which does not become suddenly 'active' like the first approach.
The thermodynamically conjugate quantity to the damage hardening variable α is denoted by (cf. Eq. (6))

$$\beta = -\frac{\partial \psi^{\text{iso}}_{\text{h}}}{\partial \alpha} = -K_1 \alpha \tag{15}$$

Using the introduced abbreviations for the thermodynamically conjugate quantitites and the constitutive assumption of Eq. (7) finally leads to the reduced dissipation inequality:

$$\mathcal{D} = \underbrace{\left(\boldsymbol{Y}_{\text{e}} - \boldsymbol{Y}^{\text{ani}}_{\text{h}}\right)}_{=\boldsymbol{Y}} : \dot{\boldsymbol{D}} + \beta \dot{\alpha} \geq 0 \tag{16}$$

At this point further constitutive equations are necessary to show that the second law of thermodynamics is truly fulfilled. These constitutive equations will be provided in the next section, where the evolution equations will be derived.

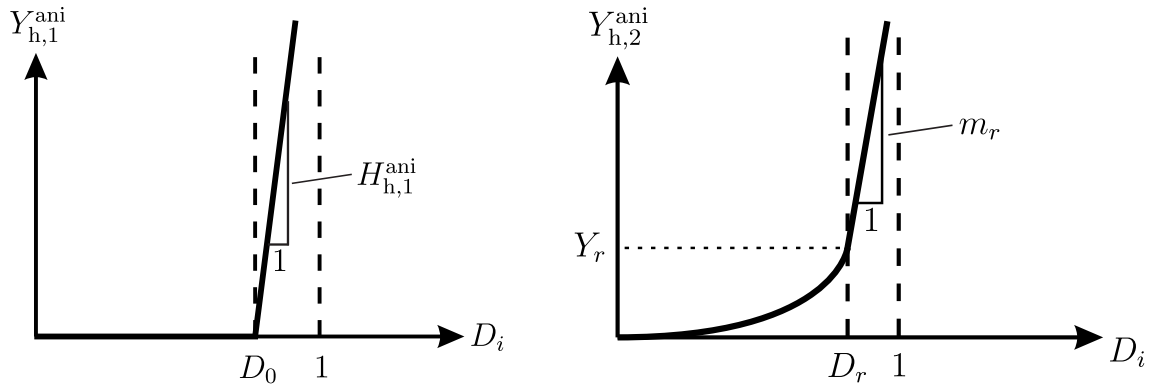

(a) suddenly increasing function $\boldsymbol{Y}^{\text{ani}}_{\text{h},1}$.

(b) smooth function $\boldsymbol{Y}^{\text{ani}}_{\text{h},2}$.

Figure 1: Schematic illustration of the two investigated anisotropic damage hardening functions $\boldsymbol{Y}^{\text{ani}}_{\text{h},1}$ and $\boldsymbol{Y}^{\text{ani}}_{\text{h},2}$.

2.3 Damage criterion and damage evolution

For the distinction between the elastic range and the damage range a damage criterion is defined. This is in analogy to plasticity models where the distinction between the elastic and the plastic range is given by the yield criterion. The damage criterion (also called damage function) is assumed to take the form

$$f = \|\boldsymbol{Y}\| - (Y_0^{\mathrm{c}} - \beta) \tag{17}$$

Here, Y_0^{c} describes the initial threshold value for the onset of damage. Noteworthy, Y_0^{c} has units of energy. Thus, the onset of damage is energetically evaluated. Following the principle of maximum dissipation yields the normality rule for the evolution equations of the internal variables $\boldsymbol{D}$ and α (associative framework)

$$\dot{\boldsymbol{D}} = \dot{\gamma}\frac{\partial f}{\partial \boldsymbol{Y}} = \dot{\gamma}\frac{\boldsymbol{Y}}{\|\boldsymbol{Y}\|} \tag{18}$$

$$\dot{\alpha} = \dot{\gamma}\frac{\partial f}{\partial \beta} = \dot{\gamma} \tag{19}$$

The corresponding Kuhn-Tucker conditions read

$$\dot{\gamma} \geq 0, \qquad f \leq 0, \qquad \dot{\gamma} f = 0 \tag{20}$$

It turns out that the damage hardening variable α can be interpreted as accumulated damage. From theoretical considerations it can be concluded that $\alpha \leq 3$ and $\|\boldsymbol{D}\| \leq \sqrt{3}$. Inserting the evolution equations into the reduced dissipation inequality (see Eq. (16)) finally yields

$$\mathcal{D} = \boldsymbol{Y} : \dot{\boldsymbol{D}} + \beta\dot{\alpha} = \boldsymbol{Y} : \dot{\gamma}\frac{\boldsymbol{Y}}{\|\boldsymbol{Y}\|} + \beta\dot{\gamma} = \dot{\gamma}\underbrace{(\|\boldsymbol{Y}\| + \beta)}_{Y_0^{\mathrm{c}}} \geq 0 \tag{21}$$

where the product $\dot{\gamma}Y_0^{\mathrm{c}}$ is always greater or equal to zero since the initial damage threshold Y_0^{c} as material parameter is assumed to be greater than zero and $\dot{\gamma} \geq 0$ (cf. Eq. 20).

2.4 Time discretization, residuals and linearization

The evolutions equations given by Eqs. (18) and (19) are discretized in time using the implicit Euler method: $\dot{\alpha}_{n+1} \approx \Delta\alpha/\Delta t$ and $\dot{\boldsymbol{D}}_{n+1} \approx \Delta\boldsymbol{D}/\Delta t$, with $\Delta\alpha = \alpha_{n+1} - \alpha_n$ and $\Delta\boldsymbol{D} = \boldsymbol{D}_{n+1} - \boldsymbol{D}_n$. Here, the indices $n+1$ and n denote the current time step and the last time step, respectively. By exploiting $\dot{\alpha} = \dot{\gamma}$ the time discretized form of Eq. (18) is given by

$$\boldsymbol{D} = \boldsymbol{D}_n + \triangle t\frac{\Delta\alpha}{\triangle t}\frac{\boldsymbol{Y}}{\|\boldsymbol{Y}\|} = \boldsymbol{D}_n + \underbrace{\Delta\alpha\frac{\boldsymbol{Y}}{\|\boldsymbol{Y}\|}}_{\Delta\boldsymbol{D}}. \tag{22}$$

where here and in the following the index $n+1$ is omitted for brevity, i.e. all quantities refer to the current time step $n+1$ if not explicitly denoted otherwise. The two considered

residuals (cf. standard plasticity models) are then

$$\boldsymbol{r}_1 = -\boldsymbol{D} + \boldsymbol{D}_n + \Delta\alpha \frac{\boldsymbol{Y}}{\|\boldsymbol{Y}\|} \tag{23}$$

$$r_2 = \|\boldsymbol{Y}\| - (Y_0^C - \beta) \tag{24}$$

This system of equations is nonlinear in the local unknowns $\boldsymbol{D}$ and α. Therefore, a linearization with respect to the local unknowns is carried out

$$\boldsymbol{r}_1 + \frac{\partial \boldsymbol{r}_1}{\partial \boldsymbol{D}} : \Delta\boldsymbol{D} + \frac{\partial \boldsymbol{r}_1}{\partial \alpha}\Delta\alpha = \boldsymbol{0} \tag{25}$$

$$r_2 + \frac{\partial r_2}{\partial \boldsymbol{D}} : \Delta\boldsymbol{D} + \frac{\partial r_2}{\partial \alpha}\Delta\alpha = 0 \tag{26}$$

This equation system with seven unknowns (six for $\Delta\boldsymbol{D}$ and one for $\Delta\alpha$) has to be solved until convergence is achieved.

3 NUMERICAL STUDIES

In order to show the behaviour of the presented anisotropic damage model in different loading cases, various strain-controlled tests at integration point level are performed. The material parameters of Table 1 are used. In total five material parameters are needed if the model with the anisotropic damage hardening $\boldsymbol{Y}_{\mathrm{h},1}^{\mathrm{ani}}$ is used and seven if the model with $\boldsymbol{Y}_{\mathrm{h},2}^{\mathrm{ani}}$ is used, where the parameter m_r is only a numerical parameter.

Symbol	Parameter	value
E	Young's modulus	100000 N/mm^2
ν	Poisson's ratio	0.3
Y_0^{c}	damage threshold	0.01 Nmm/mm^3
K_1	isotropic damage hardening parameter	0.1 Nmm/mm^3
$H_{\mathrm{h},1}^{\mathrm{ani}}$	anisotropic damage hardening parameter	10^4 Nmm/mm^3
$H_{\mathrm{h},2}^{\mathrm{ani}}$	anisotropic damage hardening parameter	1.0 Nmm/mm^3
n	anisotropic damage hardening parameter	2.0
m_r	anisotropic damage hardening parameter	10^{10} Nmm/mm^3

Table 1: Material parameters.

3.1 Uniaxial stretching

The first loading case is uniaxial stretching in x-direction, where the strain ε_{xx} is linearly increased up to 20 ‰. All the other strain components are set to zero. As mentioned

before, the situation when one eigenvalue of the damage tensor approaches the value one is critical. For this reason the two anisotropic damage hardening functions $\boldsymbol{Y}_{\mathrm{h},1}^{\mathrm{ani}}$ and $\boldsymbol{Y}_{\mathrm{h},2}^{\mathrm{ani}}$ (cf. Eqs. (13) and (14)) have been introduced. First, the behaviour of the model using the suddenly increasing function $\boldsymbol{Y}_{\mathrm{h},1}^{\mathrm{ani}}$ is discussed. The results for the normal stress components σ_{xx}, σ_{yy}, σ_{zz} and the diagonal damage components D_{xx}, D_{yy}, D_{zz} are plotted in Fig. 1a. The off-diagonal components of the stress and the damage tensor are equal to zero in this example. The stress σ_{xx} increases up to the peak load, followed by a softening up to point A, where a kink in the curve is observed. At this point the first eigenvalue of the damage tensor reaches the value $D_0 = 0.99999$. Clearly, this is the eigenvalue corresponding to the loading direction (x-direction), namely $D_1 = D_{xx}$. The values of the other two damage components D_{yy}=D_{zz}≈0.2 are still quite low. In the following path from point A to B the damage tensor is not further evolving (all components stay constant in this regime). This is intended for the damage component D_{xx} which should not further increase, but not for the components D_{yy} and D_{zz}. The damage components D_{yy} and D_{zz} do not start to increase again before they reach point B, where a second kink is observed in the curve. The reason for this behaviour can be found in the damage function $f = \|\boldsymbol{Y}\| - (Y_0^{\mathrm{c}} - \beta)$. At point A where D_{xx} reaches D_0 the xx-component of the anisotropic damage hardening force $\boldsymbol{Y}_{\mathrm{h},1}^{\mathrm{ani}}$ takes a high value since otherwise the damage in this direction would continue rising. On the other hand β only depends on α which is approximately constant at this point. At least β can not increase suddenly as $\|\boldsymbol{Y}\|$ decreases suddenly due to the anisotropic damage hardening. The consequence is an elastic region from point A to point B. At point B the elastic damage driving force $\boldsymbol{Y}_{\mathrm{e}}$ increased sufficiently enough to reproduce $f = 0$. Moreover, it can be observed that beginning from point A all normal stress components are equal. This is due to the fact that the μ-term of the stress becomes zero as soon as D_{xx} becomes 1 (cf. $\boldsymbol{\sigma}_{\mu}$ in Eq. (8)). Noteworthy, the 'penalty' parameter $H_{\mathrm{h},1}^{\mathrm{ani}}$ has to be chosen sufficiently high such that the damage tensor eigenvalues truly do not exceed the value of one. Here, already a value of $H_{\mathrm{h},1}^{\mathrm{ani}} = 10^4$ is sufficient to ensure this. Since the stress-strain curves obtained

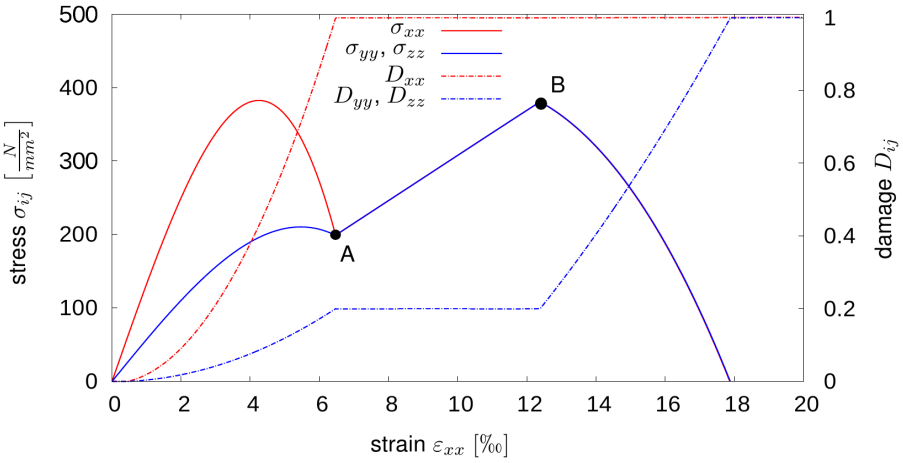

Figure 2: Uniaxial stretching using the anisotropic damage hardening $\boldsymbol{Y}_{\mathrm{h},1}^{\mathrm{ani}}$.

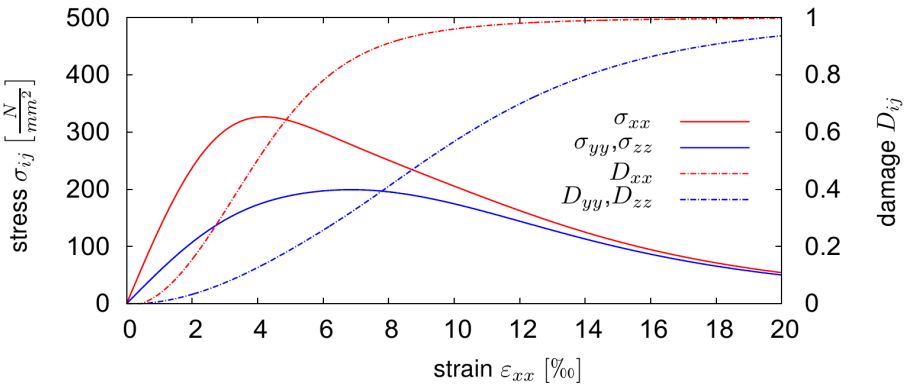

Figure 3: Uniaxial stretching using the anisotropic damage hardening $\boldsymbol{Y}_{\mathrm{h},2}^{\mathrm{ani}}$.

with the anisotropic damage hardening function $\boldsymbol{Y}_{\mathrm{h},1}^{\mathrm{ani}}$ are not satisfying due to the elastic range occuring when one eigenvalue of the damage tensor reaches one, a second approach for anisotropic damage hardening is investigated. This second function $\boldsymbol{Y}_{\mathrm{h},2}^{\mathrm{ani}}$ does not suddenly increase if a critical damage value is reached, but increases smoothly right from the beginning (cf. Fig. 1). The results for the uniaxial stretching test described above are given in Fig. 3. No kinks and elastic regions are observed and the damage components evolve without stagnating during the loading. Further, the damage components approach the value one asymptotically which was also not the case for the first presented approach. It should be noted that due to the imposed loading the stress components σ_{yy} and σ_{zz} only consist of the λ-term. This explains why the curves for these stress components approach the curve of σ_{xx} for continued loading since the stress σ_{xx} also only consists of the λ-term if the damage componnent D_{xx} has progressed close enough to one. Examiming Fig. 3 reveals that the softening slopes of the stress-strain curves are quite flat. By means of the parameter n (cf. Eq. (14)) it can be controlled how fast the anisotropic damage hardening force increases when the eigenvalues D_i approach the value one. A higher value of n leads to a delayed increase to infinity for $D_i \to 1$. Consequently, the softening slope gets steeper for higher n. Due to the demonstrated advantages of the smooth anisotropic damage hardening function, the function $\boldsymbol{Y}_{\mathrm{h},2}^{\mathrm{ani}}$ is used for the following numerical studies.

3.2 Pure shear loading

The second investigated loading case is a pure shear loading characterized by a linearly increasing shear strain ε_{xy} up to 20 ‰. All the other strain components are prescribed to be zero. The resulting stress and damage components are plotted in Fig. 4. Only the shear stress component τ_{xy} is unequal zero. The stress-strain curve shows qualitatively the same behaviour as already observed for the uniaxial stretching (cf. Fig. 3). The component D_{xy} remains unexpectedly zero, where the two diagonal components $D_{xx} = D_{yy}$ are unequal to zero and effectuate the stiffness degradation. However, this behaviour can be explained by taking into account that for the considered loading case with $\mathrm{tr}(\boldsymbol{\varepsilon}) = 0$ the elastic damage driving force $\boldsymbol{Y}_{\mathrm{e}}$ has only two entries on the main diagonal. Furthermore, the pure shear loading is identical with a biaxial tension-compression loading which can be

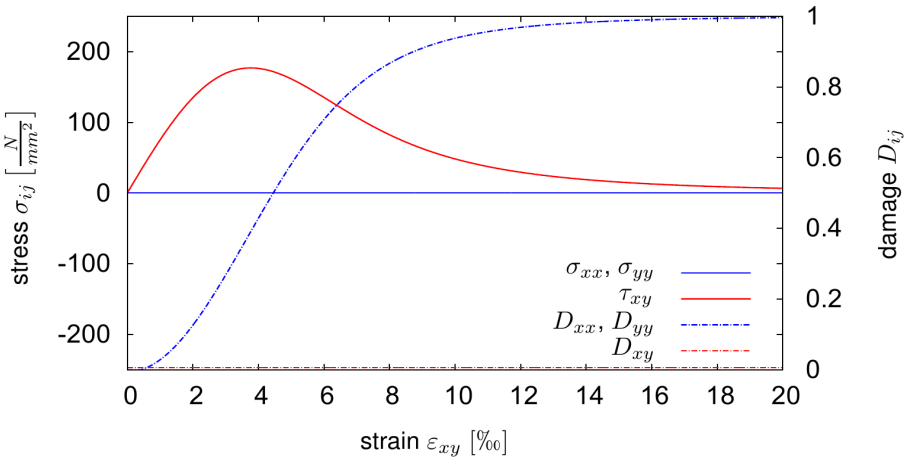

Figure 4: Pure shear loading (using the anisotropic damage hardening $\boldsymbol{Y}_{\mathrm{h},2}^{\mathrm{ani}}$).

easily shown with Mohr's circle.

3.3 Shear loading in all directions

The third investigated loading case is a loading with shear in all three components, i.e. the shear strains $\varepsilon_{xy} = \varepsilon_{yz} = \varepsilon_{xz}$ are increased at the same time up to 20 ‰. All normal strain components are set to zero. The resulting stress and damage components are plotted in Fig. 5. The shear stresses $\tau_{xy} = \tau_{yz} = \tau_{xz}$ are positive and the normal stresses are not equal to zero anymore, but are negative. This coupling between the shear strains and the normal stresses becomes apparent when Eqs. (8) and (10) are analyzed closely. Shortly before the normal stresses reach their maximum the components $D_{xy} = D_{yz} = D_{xz}$ of the damage tensor begin to decrease. This decrease can be explained by a change of the principle directions of the damage tensor during the loading which finally ends up into the state $\boldsymbol{D} = \boldsymbol{I}$. Although the components D_{xy}, D_{yz}, D_{xz} decrease during the loading, the eigenvalues of the damage rate tensor $\dot{\boldsymbol{D}}$ are always positive.

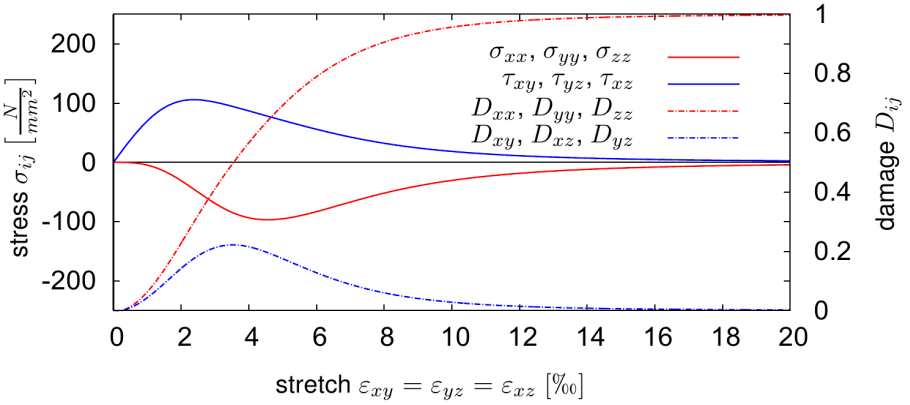

Figure 5: Shear loading in all directions (using the anisotropic damage hardening $\boldsymbol{Y}_{\mathrm{h},2}^{\mathrm{ani}}$).

4 CONCLUSIONS AND OUTLOOK

In this work an elatic anisotropic damage model for initially isotropic quasi-brittle materials has been presented. The second order damage tensor is incorporated into the elastic part of the free energy such that artificial stiffening effects can be excluded a priori. Based on the second law of thermodynamics the constitutive law as well as the evolution equations of the internal variabels are derived. Special focus was set on the bound of the eigenvalues of the damage tensor. By means of anisotropic damage hardening it is ensured that the eigenvalues do not exceed the value one. Eigenvalues greater than one are not physical and would cause numerical troubles in addition. Two approaches for the anisotropic damage hardening force are investigated: (i) a suddenly increasing function and (ii) a smooth function. Exemplarily, it was shown with an uniaxial stretching test that the first approach suffers from a spurious second elastic region which arises when the first eigenvalue reaches one. The second approach with the smooth function performs well and provides the desired stress-strain curves with continued softening at the critical points characterized by $D_i \to 1$. Two more numerical examples (pure shear and shear in all directions) demonstrate the behaviour of the model in two- and three-dimensional loading cases.
It is commonly known that using finite element analysis in combination with standard (local) damage models leads to mesh-sensitive results. Damage localizes into one element row which leads to vanishing dissipation if the element size tends to zero. In order to overcome this situation, a gradient extension of the presented model is pursued, which will be described in detail in [11]. Moreover, future work will deal with the incorporation of crack-closure (unilateral effect) as well as the consideration of anisotropic materials.

REFERENCES

[1] Kachanov, L.M. Time of the rupture process under creep conditions. *Izy Akad. Nank SSR Otd Tech Nauk* (1958) **8**:26–31.

[2] Kuhl, E. and Ramm, E. On the linearization of the microplane model. *Mechanics of Cohesivefrictional Materials* (1998) **3**(4):343–364.

[3] Kachanov, L.M. *Introduction to continuum damage mechanics (Vol. 10)*. Springer Science and Business Media, 2013.

[4] Cordebois, J.P. and Sidoroff, F. Damage induced elastic anisotropy In: *Mechanical Behavior of Anisotropic Solids* (pp.761–774), Springer, 1982.

[5] Murakami, S. *Continuum damage mechanics: a continuum mechanics approach to the analysis of damage and fracture (Vol. 185)*. Springer Science and Business Media, 2012.

[6] Fassin, M., Wulfinghoff, S. and Reese, S. Different Numerical Time Integration Schemes for elastoplasticity coupled to anisotropic damage. In: *Applied Mechanics and Materials* (Vol. 784, pp. 217–224) Trans Tech Publications, 2015.

[7] Wulfinghoff, S., Fassin, M. and Reese, S. Comparison of Two Time-Integration Algorithms for an Anisotropic Damage Model Coupled With Plasticity. In: *Applied Mechanics and Materials* (Vol. 784, pp. 292–299) Trans Tech Publications, 2015.

[8] Chaboche, J.L. Anisotropic creep damage in the framework of continuum damage mechanics. *Nuclear engineering and design* (1984) **79**(3):309–319.

[9] Wulfinghoff, S., Fassin, M. and Reese, S. A damage growth criterion for anisotropic damage models motivated from micromechanics. *International Journal of Solids and Structures* (2017) **121**:21–32.

[10] Fassin, M., Wulfinghoff, S. and Reese, S. A gradient-extended elastic isotropic damage model considering crack-closure. *Proceedings of the 7th GACM Colloquium on Computational Mechanics for Young Scientists from Academia and Industry* (2017), pp. 305–311.

[11] Wulfinghoff, S., Fassin, M. and Reese, S. A framework for anisotropic gradient-extended models of brittle damage and fracture. *in preparation* (2018).